

Published in final edited form as:

*Ann Neurol.* 2011 October ; 70(4): 646–656. doi:10.1002/ana.22528.

## Toll-like Receptor 4 Contributes to Poor Outcome after Intracerebral Hemorrhage

Lauren H. Sansing, M.D., M.S.T.R.<sup>1,2</sup>, Tajie H. Harris, Ph.D.<sup>3</sup>, Frank A. Welsh, Ph.D.<sup>4</sup>, Scott E. Kasner, M.D., M.S.C.E.<sup>1</sup>, Christopher A. Hunter, Ph.D.<sup>3</sup>, and Katalin Kariko, Ph.D.<sup>4</sup>

<sup>1</sup>Department of Neurology, School of Medicine, University of Pennsylvania

<sup>2</sup>Departments of Neurology and Neuroscience, University of Connecticut Health Center and Departments of Neurology and Neurosurgery, Hartford Hospital (current)

<sup>3</sup>Department of Pathobiology, School of Veterinary Medicine, University of Pennsylvania

<sup>4</sup>Department of Neurosurgery, School of Medicine, University of Pennsylvania

### Abstract

**Objective**—Intracerebral hemorrhage (ICH) is a devastating stroke subtype in which perihematomal inflammation contributes to neuronal injury and functional disability. Histologically, the region becomes infiltrated with neutrophils and activated microglia followed by neuronal loss but little is known about the immune signals that coordinate these events. This study aimed to determine the role of Toll-like receptor 4 (TLR4) in the innate immune response after ICH and its impact on neurobehavioral outcome.

**Methods**—Transgenic mice incapable of TLR4 signaling and wild-type controls were subjected to striatal blood injection to model ICH. The perihematomal inflammatory response was then quantified by immunohistochemistry, whole brain flow cytometry, and PCR. The critical location of TLR4 signaling was determined by blood transfer experiments between genotypes. Functional outcomes were quantified in all cohorts using the cylinder and open field tests.

**Results**—TLR4-deficient mice had markedly decreased perihematomal inflammation, associated with reduced recruitment of neutrophils and monocytes, fewer microglia, and improved functional outcome by day 3 after ICH. Moreover, blood transfer experiments revealed that TLR4 on leukocytes or platelets within the hemorrhage contributes to perihematomal leukocyte infiltration and the neurological deficit.

**Interpretation**—Together, these data identify a critical role for TLR4 signaling in perihematomal inflammation and injury and indicate this pathway may be a target for therapeutic intervention.

### Introduction

Intracerebral hemorrhage (ICH) is a devastating stroke subtype caused by rupture of penetrating arteries within the brain, usually due to hypertension. Approximately two million cases of ICH occur worldwide each year<sup>1</sup> and patients presenting with ICH have nearly twice the risk of being severely disabled compared to patients with ischemic stroke<sup>2</sup>. Despite these statistics, there is no specific treatment for ICH<sup>3</sup> and mortality has not improved over recent decades<sup>4,5</sup>. Multiple studies have described the presence of an intense local inflammatory response surrounding the hemorrhage and have implicated this immune

response in the pathogenesis of secondary injury after ICH<sup>6</sup>. In the days following ICH, activation of the innate immune system leads to local cytokine production<sup>7, 8</sup>, neutrophil infiltration<sup>9</sup>, microglial activation, and progressive neuronal loss<sup>10</sup> which likely contributes to poor outcome. Understanding the events that initiate or propagate the inflammatory response may lead to therapies that improve clinical outcomes.

The activation of an innate immune response culminates in the production of pro-inflammatory cytokines and chemokines. Toll-like receptors (TLRs) recognize pathogen- and damage-associated molecular patterns and have a key role in innate immunity<sup>11</sup>. While TLRs are critical for host responses to pathogens, they also contribute to the development of sterile inflammation. Specifically, Toll-like receptor 4 (TLR4) is activated by a number of endogenous proteins that act as “danger signals” in the setting of injury. Many of these endogenous TLR4 ligands, including heme<sup>12</sup>, fibrinogen<sup>13</sup>, HSP70<sup>14</sup>, hyaluronan<sup>15</sup>, and high-mobility group box 1<sup>16</sup> are present in the brain after ICH. Moreover, in the central nervous system (CNS), microglia and some neurons express TLR4 and when stimulated increase cytokine and chemokine production and sustain CNS inflammation independent of blood-derived leukocytes<sup>17, 18</sup>. In ICH, TLR4 was recently shown to be upregulated 6 hours through 3 days in a rat model<sup>19</sup>, but the functional significance of this is unknown. In models of ischemic stroke, mice deficient in TLR4 have lower inducible nitric oxide synthase and matrix metalloproteinase-9 (MMP-9) expression and smaller infarct volumes compared to wild-type<sup>20</sup>. Thus, there are considerable data implicating TLR4 in sterile inflammation in the CNS. However, while TLR4 is implicated in ischemic stroke, the triggers of the immune response are distinct in ICH (e.g. thrombin, hemoglobin degradation products) and the role of TLR4 is unknown. In this study, the autologous blood injection model of ICH<sup>21</sup> was utilized to assess the role of TLR4 in the innate immune response *in vivo* and how it influences functional outcome. The results identified a major role for TLR4 in the pathological deficits observed after ICH and indicate this pathway may be a target for therapeutic inhibition.

## Methods

### Mice

Male TLR4-deficient (C3H/HeJ) and wild-type (WT, C3H/HeOuJ) mice from Jackson Laboratory (Bar Harbor, ME), aged 14–18 weeks, were used for TLR4 experiments. The TLR4-deficient mice have a C to A substitution in the third exon of the Toll-like receptor 4 gene on chromosome 4, which replaces proline with histidine and renders the receptor incapable of signal transduction<sup>22</sup>. Male C57BL/6N and B6LY5.2/Cr from Charles River NCI-Frederick APA were used for the CD45.1/CD45.2 blood transfer experiment. All experiments were carried out with the approval of the IACUC of the University of Pennsylvania and/or the University of Connecticut Health Center.

### Intracerebral hemorrhage surgery

Mice were anesthetized with inhaled 70% N<sub>2</sub>O, 30% O<sub>2</sub>, and 1–3% Isoflurane with buprenorphine 0.1mg/kg SC for analgesia. 15 µL arterial blood was injected at 0.5 µL/min by microinfusion pump (WPI, Sarasota, FL) at 2.5 mm right of bregma, 5° medial and 3 mm deep without antithrombotic agents while body temperature was maintained at 37 ± 0.5°C. Sham surgeries included all procedures (including needle insertion) except blood injection. For the various experiments, autologous blood or blood from a donor was injected into WT or TLR4-deficient mice. ICH success was judged based on inspection of a coronal section at the needle insertion site, blinded to genotype. Hemorrhages that tracked down to the base of the brain, up the needle track past the corpus callosum, or into the ventricles were deemed unsuccessful and that mouse was eliminated from all analyses. ICH success rate was 80%.

Assessment of source of perihematomal leukocytes by flow cytometry: C57BL/6N (homozygous for the CD45.2 allele) mice were used as blood donors for ICH surgery on B6LY5.2/Cr mice (homozygous for the CD45.1 allele). Mice were sacrificed at 24 and 72 hours and brains analyzed by flow cytometry for the source of the measured leukocyte populations.

### Quantification of neurobehavioral deficit

Cylinder testing was performed post-operatively each morning by an observer blinded to genotype/treatment. Each mouse was placed in a 12-cm diameter clear glass cylinder, observed for 20 rears, and initial placement of the forelimbs on the wall of the cylinder was scored per rear. Subsequent movements (such as lateral exploration) were not scored. The laterality index was calculated as  $(\# \text{ right forelimb placements} - \# \text{ left placements}) / (\# \text{ right} + \# \text{ left} + \# \text{ both})$ , where 0 indicated no forelimb preference and 1 indicated the left forelimb was never placed<sup>23</sup>.

Open field testing was performed to measure total spontaneous locomotor activity in a novel environment<sup>24</sup>. In the morning on day 3 post-ICH, each mouse was allowed to acclimate to the dark room for 10 minutes and then placed in the open field chamber (16" × 16" field with photobeam grid). Total motility was quantified as the total number of beam breaks in a 20 minute session using the automated PAS Open Field system (San Diego Instruments, San Diego, CA). Testing was performed blinded to genotype/treatment.

### Immunohistochemistry

Mice were euthanized at  $72 \pm 2$  hours after ICH and brains immediately frozen in Tissue-tek O.C.T. (Andwin Scientific, Addison, IL) and stored at  $-80^{\circ}\text{C}$ . 6  $\mu\text{m}$  fixed and blocked sections were incubated with rat anti-mouse Ly6G (5  $\mu\text{g}/\text{mL}$ ) or rat anti-mouse CD11b (2.5  $\mu\text{g}/\text{mL}$ ) (eBioscience, San Diego, CA) followed by Cy3 Affinipure goat anti-rat IgG (Jackson Immunoresearch, West Grove, PA), at 1:500. DAPI was used at 0.5  $\mu\text{g}/\text{mL}$  (Roche Diagnostics, Mannheim, Germany).

Images were acquired using a Nikon E600 fluorescence microscope with NIS Elements software (Nikon, Melville, NY). On post-ICH day 3, the area of hematoma was evident as a paucicellular (by DAPI nuclear staining) region with disrupted extracellular matrix. In each of five mice, five representative ROI's adjacent to the hematoma were chosen for cell quantification by an observer blinded to mouse genotype and high resolution photomicrographs were taken and enlarged for cell counting (also performed blinded to genotype). Neutrophil infiltration was quantified by summing the number of Ly6G+ cells in five perihematomal 40x fields per mouse. CD11b+ cells were quantified by summing the number of positive cells in five 20x fields, with large, vacuolated cells defined as having at least one diameter  $> 10 \mu\text{m}$  with clear cytoplasm.

### Tissue preparation for flow cytometry

Immediately following sacrifice, 1 mL blood was collected into heparin 200 U/mL then mice were perfused with 40 ml of ice-cold PBS and the brains and spleens removed. The two cerebral hemispheres were divided along the interhemispheric fissure; each hemisphere was placed in complete RPMI 1640 (Life Technologies, Gaithersburg, MD) medium and processed as we have previously described<sup>25</sup>.

Heparinized blood was overlaid on 4 mL Lympholyte-M, centrifuged at 800xg and leukocytes harvested from the interphase. Spleens were pressed through a 70  $\mu\text{m}$  strainer, suspended in complete RPMI and pelleted at 1600xg for 5 min. Red blood cells were lysed with 0.86%  $\text{NH}_4\text{Cl}$ .

## Flow cytometry

Cells were washed in PBS and then blocked with 50  $\mu$ L Fc block (10% CD16/CD32 10  $\mu$ g/mL, BD Biosciences, 0.5% normal rat IgG in FACS buffer (1 $\times$  PBS, 0.2% BSA, and 2 mM EDTA)) for 15 minutes prior to staining with CD45-APC, CD11b-PerCp Cy5.5, CD11c-PECy7, CD3-FITC, CD19-FITC, NK1.1-FITC, Gr-1-PE (all eBioscience), and Ly6G-v450 (BD Horizon) for 15 minutes. For the CD45.1/CD45.2 experiments the panel was CD45.2-FITC (BD Pharmingen), CD3-v500 (BD Horizon), CD19-Qdot655 (Invitrogen), Ly6G-v450, CD11c-PECy7, CD45.1-PE, Gr-1-PerCp Cy5.5, and CD11b-eFluor780 (eBioscience). Data was acquired on a BD Canto II or LSR II using FACSDIVA 6.0 (BD Biosciences) and analyzed using FlowJo (Treestar Inc., Ashland, OR). Hematopoietic cells were identified as CD45<sup>hi</sup>, neutrophils as CD45<sup>hi</sup>CD3<sup>-</sup>CD19<sup>-</sup>NK1.1<sup>-</sup>CD11b<sup>+</sup>Ly6G<sup>+</sup>, monocytes as CD45<sup>hi</sup>CD3<sup>-</sup>CD19<sup>-</sup>NK1.1<sup>-</sup>CD11b<sup>+</sup>Ly6G<sup>-</sup>CD11c<sup>-</sup>Gr-1<sup>-</sup>, inflammatory monocytes as CD45<sup>hi</sup>CD3<sup>-</sup>CD19<sup>-</sup>NK1.1<sup>-</sup>CD11b<sup>+</sup>Ly6G<sup>-</sup>CD11c<sup>-</sup>Gr-1<sup>+</sup>, and dendritic cells as CD45<sup>hi</sup>CD3<sup>-</sup>CD19<sup>-</sup>NK1.1<sup>-</sup>CD11b<sup>+</sup>Ly6G<sup>-</sup>CD11c<sup>+</sup>. Microglia were identified as CD45<sup>int</sup>CD11b<sup>+</sup>. All experiments were replicated at least three times on different days with populations gated based on fluorescence minus one (FMO) controls.

## Relative quantitative real-time PCR analysis

Total RNA was extracted from a 36 mm<sup>3</sup> section of perihematomal brain and a corresponding section of the contralateral hemisphere after sham and ICH surgeries in WT and TLR4-deficient mice sacrificed at 24 and 72 hours using RNeasy lipid tissue mini kit (Qiagen, Valencia, CA). Random-primed cDNA was synthesized using MMLV reverse transcriptase (Invitrogen, Carlsbad, CA). Expression of inflammatory cytokines (IL-1 $\beta$  and IL-6), chemokines/receptors involved in neutrophil and monocyte recruitment (CCR1, CXCR1, CX3CL1, CCR2, CSF2, and CXCL1), a marker for alternatively-activated macrophages (arginase), a scavenger receptor involved in phagocytosis after ICH (CD36), and MMP-9 were determined using an AB7500 fast real-time PCR thermal cycler and power SYBR green reagents (Applied Biosystems, Foster City, CA). HPRT was used as normalization control. Commercially available Quantitect primers (Qiagen, Valencia, CA) were used except for CCR2 (forward: CCA CAC CCT GTT TCG CTG TA, reverse: TGC ATG GCC TGG TCT AAG TG) and IL-10 (forward: GGT TGC CAA GCC TTA TCG GA, reverse: ACC TGC TCC ACT GCC TTG CT). Gene expression relative to the contralateral hemisphere of a sham mouse at 24 hours was calculated using the ddCT method.

## Statistical analysis

Cell counts by were tested for normality and differences between groups compared by two-sided t-test or Wilcoxon rank sum with correction for multiple comparisons where appropriate. For blood-derived leukocyte populations the excess ipsilateral cells (# ipsilateral - # contralateral) cells in the brain were calculated so that the uninjured hemisphere of each mouse served as an internal control for the success of perfusion in each mouse. Ipsilateral microglia counts were reported directly. Cylinder test results were compared by ANOVA followed by t-tests since the comparisons were pre-specified and distribution was normal. Analysis was performed with Stata IC/10 (College Station, TX).

## Results

### A role for TLR4 in the perihematomal inflammatory infiltrate

To determine the possible role of TLR4 in the pathology after ICH, the inflammatory infiltrate was characterized at several time-points post-ICH in WT and TLR4-deficient mice. The use of immunohistochemistry to quantify the total numbers of all CD11b<sup>+</sup> cells revealed no difference between WT and TLR4-deficient mice (Figures 1A and 1B). Since most

CD11b<sup>+</sup> cells in the brain are microglia, this suggested that TLR4 did not profoundly affect perihematomal microglial numbers. However, WT mice had more large, vacuolated CD11b<sup>+</sup> cells (Figure 1C) and neutrophils (Figures D–F) than the TLR4-deficient mice indicating a difference in the leukocyte subtypes within the CD11b<sup>+</sup> (myeloid) population between the genotypes.

To further quantify how TLR4 affected the specific myeloid populations in the ipsilateral and contralateral hemispheres, the flow cytometry gating strategy shown in Figure 2A was developed. There was no difference in the number of each cell type in the contralateral hemisphere by genotype or post-ICH day. However, ipsilateral blood-derived leukocytes increased by four-fold in WT mice between days 1 and 3 post-ICH, while the TLR4-deficient mice had fewer leukocytes on both days (Figure 2B). Ipsilateral neutrophils increased five-fold in WT mice between days 1 and 3 post-ICH, but in the absence of TLR4 signaling the neutrophils were reduced by 75% on day 3 post-ICH (Figure 2C). Ipsilateral monocytes increased ten-fold in the three days after ICH in WT mice but this population was also reduced by approximately 75% in the TLR4-deficient mice on day 3 post-ICH (Figure 2D). Inflammatory monocytes (Figure 2E) also increased dramatically in the ipsilateral hemisphere over time and were reduced by 50% in the TLR4-deficient mice on day 3 post-ICH. Dendritic cells (Figure 2F) also increased in the ipsilateral hemisphere but without differing between the genotypes. These differences between WT and TLR4-deficient mice were not reflected in the periphery (Table 1).

In order to confirm that the leukocyte populations measured were infiltrating from the periphery and not residual leukocytes from the injected ICH, blood from CD45.2 (C57BL/6N) mice was used to create ICH in CD45.1 (B6LY5.2/Cr) mice and the brains analyzed by flow cytometry on days 1 and 3 post-ICH for the source of the leukocyte populations. On day 1 post-ICH, the vast majority of CD45<sup>+</sup> cells were CD45.1, indicating they derived from the recipient mouse's peripheral blood, while only 10% of the cells carried CD45.2, indicating they originated from the injected ICH (Figure 3A and C). By day 3 post-ICH, almost no live injected (CD45.2) leukocytes remained (Figure 3B and C).

Microglia were identified as CD45<sup>int</sup>CD11b<sup>+</sup> cells (gating shown in Figure 4A). Microglia numbers increased from days 1 to 3 post-ICH in both genotypes but significantly less so in the TLR4-deficient mice (Figure 4B). Together, these data identify suggest the initial recruitment of dendritic cells is TLR4-independent but that TLR4 participates in neutrophil, monocyte, and inflammatory monocyte recruitment and the proliferation and/or recruitment of microglia to the perihematomal brain.

### Analysis of local inflammatory gene expression in ICH

To further characterize the inflammatory response after ICH, cytokine and chemokine gene expression was examined by quantitative real-time PCR. In WT mice, ICH resulted in the local upregulation of IL-1 $\beta$ , IL-6, CCR1, CCR2, CXCL1, and CD36 at 24 and 72 hours. CX3CL1 was upregulated in both hemispheres at 24 hours but not at 72 hours, while CSF2 and arginase were upregulated ipsilaterally at 72 hours (Supplemental Table 1).

In the TLR4-deficient mice, CD36 expression was higher at 24 hours compared to WT (Figure 5A). Both CSF2 and CX3CL1 were increased in TLR4-deficient mice at 72 hours compared to WT. The transcription levels of the remainder of the gene products were similar between the genotypes, suggesting that TLR4 is not involved in their transcriptional response to injury. Interestingly, the increases in CD36, CSF2 and CX3CL1 in the TLR4-deficient mice suggest a role for TLR4 in their regulation after injury.



### Impact of TLR4 on motor function after ICH

In order to test the contribution of TLR4 to the functional deficits after ICH, TLR4-deficient and WT mice were subjected to daily neurobehavioral testing. As injection of blood into the right striatum results in left pure motor hemiparesis, the cylinder test<sup>23</sup> was used to quantify motor function as displayed by the preferential use of the right forelimb upon rearing. Sham mice were also tested to quantify the injury due to the surgery and needle insertion. After ICH, both genotypes had the same degree of right forelimb preference on the cylinder test on day 1 (Figure 5B), suggesting that TLR4 did not influence the initial injury. However, WT mice had progressively decreased use of the left forelimb (and therefore higher laterality index) over the next three days, presumably as a consequence of inflammation and secondary injury at the site of ICH. In contrast, the TLR4-deficient mice improved to the same functional level as the sham mice by day 3. On day 3 post-ICH the mice were also tested on the open field to quantify overall locomotor activity. The TLR4-deficient mice had significantly more beam breaks (and therefore greater motility) than WT mice (Figure 5B). The improvement in functional outcome in TLR4-deficient mice observed in two independent outcome measures is consistent with the reduced inflammation observed in Figures 1 and 2 and suggests that the local TLR4-induced inflammatory response contributes to neurobehavioral deficits.

### TLR4 within the hemorrhage mediates the inflammatory response

While the above studies highlight a role for TLR4 post-ICH, it was unclear if the critical source of TLR4 signaling was resident CNS cells and/or the cellular components within the hemorrhage. Therefore, in an attempt to distinguish the relative contribution of TLR4 in these distinct compartments, blood transfer experiments were performed in which TLR4-deficient blood was injected into the brains of WT mice and WT blood was injected into the brains of TLR4-deficient mice. The perihematomal infiltrates and behavioral effect were then quantified. Compared to WT mice with an ICH composed of WT blood, WT mice with an ICH composed of TLR4-deficient blood had fewer total infiltrating leukocytes, inflammatory monocytes, monocytes and microglia and a trend toward reduced neutrophils (Figure 6). The TLR4-deficient mice given an ICH composed of WT blood had more ipsilateral infiltrating leukocytes and monocytes than the TLR4-deficient mice with a TLR4-deficient ICH. Dendritic cell counts did not differ when the mice were given ICH of a different TLR4 genotype. These data suggest that the recruitment of the monocyte and inflammatory monocyte populations are stimulated by TLR4-dependent signals from cells within the ICH.

The functional effect of hemorrhages composed of leukocytes of the different genotypes was examined by subjecting the mice to daily cylinder testing as described above. All cohorts had similar deficits on day 1 post-ICH, confirming that TLR4 was not an important contributor to the severity of the initial injury. However, like the WT mice given autologous blood injection, the TLR4-deficient mice given an ICH with WT blood continued to show severe behavioral deficits on day 3 post-ICH. The WT mice given an ICH with TLR4-deficient blood had minimal deficits, similar to the TLR4-deficient mice with an autologous ICH (Figure 7). Consistent with these results, the WT mice with an ICH composed of TLR4-deficient blood showed higher locomotor activity than the TLR4-deficient mice with a WT ICH on open field testing. These results indicate that TLR4 activation of the cells within the hemorrhage contributes to the detrimental inflammatory response and sustained neurologic deficit in the days after ICH.

## Discussion

Current models of ICH suggest that activation of the innate immune system leads to inflammation and secondary brain injury resulting in neuronal death, edema, and neurological deterioration<sup>6, 26</sup> but little is known about the role of TLRs in this process. Increases in ipsilateral blood-derived leukocytes, neutrophils, monocytes, inflammatory monocytes, dendritic cells and microglia were demonstrated between days 1 and 3 after striatal autologous blood injection in WT mice. Our work builds on a prior study that similarly used flow cytometry to quantify the inflammatory response after ICH and demonstrated an increase in blood-derived leukocytes in the days after ICH surgery<sup>27</sup>.

These studies used the double blood injection model of ICH, which produces a striatal hemorrhage that mimics a hypertensive ICH in humans. A limitation of this model is that it does not directly model the rupture of a diseased blood vessel that causes a spontaneous human ICH. The most common other mouse model of ICH involves injection of bacterial collagenase into the striatum, which may directly affect the inflammatory response and thus was not used for these immunological investigations.

Using this system, the role of TLR4-mediated inflammation in secondary neuronal injury was determined *in vivo*. Transgenic mice that lack functional TLR4 were found to have fewer ipsilateral blood-derived leukocytes, neutrophils, monocytes, and inflammatory monocytes on day 3 post-ICH compared to the WT controls, but the changes in the perihematomal inflammatory infiltrate did not merely mirror the systemic inflammatory response. This suggests that the TLR4-dependence of the chemotactic signal is likely localized to the brain.

The functional deficit on day 1 post-ICH did not differ between genotypes, consistent with the hypothesis that initial injury is caused by mechanical disruption of neurons and glia rather than inflammation<sup>1</sup>. Importantly, the TLR4-deficient mice demonstrated improved functional outcome as well as a diminished inflammatory infiltrate indicating that events downstream of TLR4 are involved in leukocyte recruitment to the brain and that these cells contribute to perihematomal injury and the progressive neurological deficit seen in the WT mice.

One of the major findings to emerge from this model was that the presence of TLR4 in blood, not on the resident CNS cells, was the critical factor that contributed to neurological injury. This suggests that ICH leads to local activation of TLR4 on platelets or leukocytes within the hemorrhage, perhaps via fibrinogen/fibrin within the clot, and this promotes the inflammation and results in poor functional outcome. Alternatively, degranulating neutrophils within the ICH may directly release substances (e.g. myeloid related protein 8/14<sup>28</sup>) or degrade extracellular matrix proteins (e.g. hyaluronic acid, fibronectin, and/or heparin sulfate<sup>29</sup>) that activate TLR4 on the neighboring intrahematomal leukocytes leading to excess inflammation. The role of TLR4 on the cellular components within the cerebral hematoma in mediating the inflammatory response and neurological deficit had not previously been identified.

The consistent finding of improved functional outcome and reduced infiltrating neutrophils in the TLR4-deficient mice and the WT mice with a TLR4-deficient ICH suggests that neutrophils may directly contribute to perihematomal injury. However, other myeloid populations were decreased in the TLR4-deficient mice as well. Microglia, monocytes and inflammatory monocytes likely contribute to acute injury by releasing inflammatory cytokines and chemokines or may contribute to recovery by aiding in phagocytosis of cellular debris or by shifting response to a less inflammatory one. Additional studies will be

required to elucidate the role of infiltrating neutrophil and monocyte populations and microglia in the perihematomal region.

Interestingly, CX3CL1 (fractalkine), CSF2, and CD36 were increased in the TLR4 mice compared to WT. Soluble CX3CL1 is a potent chemoattractant for T cells, NK cells, and monocytes<sup>30–32</sup>, however CX3CL1 also exists in a membrane-bound form on neurons and interacts with CX3CR1 on microglia<sup>33, 34</sup>. An emerging neuroprotective role is being elucidated for CX3CL1 in the setting of acute inflammatory stimuli in various CNS injury models<sup>35–38</sup>. Similarly, the hematopoietic growth factor CSF2 (GM-CSF) has recently been shown to have neuroprotective effects in stroke and Parkinson's disease<sup>39–42</sup>. In addition, recent work has demonstrated an important role for microglial CD36 expression in the resolution of ICH in a mouse model<sup>43</sup>. CD36 is a scavenger receptor expressed on microglia and macrophages (among other cell types) and mediates the phagocytosis of red blood cells and apoptotic cells, which is likely beneficial in acute ICH. In contrast, cerebral ischemia stimulates CD36 leading to activation of NF- $\kappa$ B, inflammatory gene expression, and larger infarcts<sup>44</sup>. In this paradigm CD36 signals in a complex with activated TLR2/1, while CD36 did not mediate inflammation after TLR4 stimulation<sup>45</sup>. In accordance with these findings, macrophage CD36-mediated phagocytosis of red blood cells did not induce an inflammatory response in the absence of TLR2 stimulation in a model of malaria<sup>46</sup> and in fact, human monocyte populations reduced inflammatory cytokines IL-1 $\beta$  and TNF- $\alpha$  when treated with apoptotic neutrophils and T cells to activate CD36 after TLR4 (LPS) stimulation<sup>47</sup>. Thus the effect of CD36 activation may depend on the costimulatory signals. It is possible that upregulation of CX3CL1, CSF2, and/or CD36 in the TLR4-deficient mice may have a role in their improved neurological outcome, although each needs further study before conclusions can be drawn. It was surprising that the TLR4-deficient mice had no reduction in most of the inflammatory gene expression in perihematomal brain at 24 and 72 hours. Cytokines contributing to perihematomal inflammation may not be transcriptionally regulated (e.g. IL-1 $\beta$ ) or other chemokines may be important for leukocyte migration (e.g. C5a). Alternatively, detection of changes in transcription in small numbers of relevant cells may have been limited when examining the entire perihematomal region.

In summary, these studies have elucidated a previously unknown role for TLR4 in the development of perihematomal inflammation and secondary injury after ICH. This suggests that therapeutic inhibition of TLR4 signaling in the acute phase after ICH may lead to improved clinical outcomes for this devastating type of stroke. The clinical relevance is great, as a synthetic TLR4 antagonist has been developed (E5564, eritoran, Eisai Pharmaceuticals) and completed clinical trials for sepsis. In addition, the data identify chemotactic signals downstream of TLR4 as potential therapeutic targets.

## Supplementary Material

Refer to Web version on PubMed Central for supplementary material.

## Acknowledgments

The work was supported by a fellowship from the Institute of Translational Medicine and Therapeutics from the University of Pennsylvania and the Marlene L. Cohen and Jerome H. Fleisch Scholar Grant (LHS), T32-AI-055400 and AI-081478 (THH), NS-29331 (FAW) and AI41158 (CAH).

## References

1. Qureshi AI, Mendelow AD, Hanley DF. Intracerebral haemorrhage. *Lancet*. 2009; 373:1632–1644. [PubMed: 19427958]



2. Chiu D, Peterson L, Elkind MSV, et al. Comparison of Outcomes after Intracerebral Hemorrhage and Ischemic Stroke. *Journal of Stroke and Cerebrovascular Diseases*. 2010; 19:225–229. [PubMed: 20434051]
3. Morgenstern LB, Hemphill JC 3rd, Anderson C, Becker K, Broderick JP, Connolly ES Jr, Greenberg SM, Huang JN, Macdonald RL, Messé SR, Mitchell PH, Selim M, Tamargo RJ. on behalf of the American Heart Association Stroke Council and Council on Cardiovascular Nursing. Guidelines for the Management of Spontaneous Intracerebral Hemorrhage: A Guideline for Healthcare Professionals From the American Heart Association/American Stroke Association. *Stroke*. 2010; 41:2108–2129. [PubMed: 20651276]
4. Flaherty ML, Haverbusch M, Sekar P, et al. Long-term mortality after intracerebral hemorrhage. *Neurology*. 2006; 66:1182–1186. [PubMed: 16636234]
5. van Asch CJ, Luitse MJ, Rinkel GJ, et al. Incidence, case fatality, and functional outcome of intracerebral haemorrhage over time, according to age, sex, and ethnic origin: a systematic review and meta-analysis. *Lancet Neurol*. 2010; 9:167–176. [PubMed: 20056489]
6. Wang J, Dore S. Inflammation after intracerebral hemorrhage. *J Cereb Blood Flow Metab*. 2007; 27:894–908. [PubMed: 17033693]
7. Hua Y, Wu J, Keep RF, et al. Tumor necrosis factor- $\alpha$  increases in the brain after intracerebral hemorrhage and thrombin stimulation. *Neurosurgery*. 2006; 58:542–550. discussion 542-550. [PubMed: 16528196]
8. Carmichael ST, Vespa PM, Saver JL, et al. Genomic profiles of damage and protection in human intracerebral hemorrhage. *J Cereb Blood Flow Metab*. 2008; 28:1860–1875. [PubMed: 18628781]
9. Gong C, Hoff JT, Keep RF. Acute inflammatory reaction following experimental intracerebral hemorrhage in rat. *Brain Research*. 2000; 871:57–65. [PubMed: 10882783]
10. Wasserman JK, Schlichter LC. Neuron death and inflammation in a rat model of intracerebral hemorrhage: Effects of delayed minocycline treatment. *Brain Research*. 2007; 1136:208–218. [PubMed: 17223087]
11. Akira S, Uematsu S, Takeuchi O. Pathogen Recognition and Innate Immunity. *Cell*. 2006; 124:783–801. [PubMed: 16497588]
12. Figueiredo RT, Fernandez PL, Mourao-Sa DS, et al. Characterization of heme as activator of Toll-like receptor 4. *J Biol Chem*. 2007; 282:20221–20229. [PubMed: 17502383]
13. Smiley ST, King JA, Hancock WW. Fibrinogen stimulates macrophage chemokine secretion through toll-like receptor 4. *J Immunol*. 2001; 167:2887–2894. [PubMed: 11509636]
14. Vabulas RM, Ahmad-Nejad P, Ghose S, et al. HSP70 as endogenous stimulus of the Toll/interleukin-1 receptor signal pathway. *J Biol Chem*. 2002; 277:15107–15112. [PubMed: 11842086]
15. Termeer C, Benedix F, Sleeman J, Fieber C, Voith U, Ahrens T, Miyake K, Freudenberg M, Galanos C, Simon JC. Oligosaccharides of Hyaluronan Activate Dendritic Cells via Toll-like Receptor 4. *The Journal of Experimental Medicine*. 2002; 195:95–111.
16. Park JS, Svetkauskaite D, He Q, et al. Involvement of toll-like receptors 2 and 4 in cellular activation by high mobility group box 1 protein. *J Biol Chem*. 2004; 279:7370–7377. [PubMed: 14660645]
17. Olson JK, Miller SD. Microglia Initiate Central Nervous System Innate and Adaptive Immune Responses through Multiple TLRs. *J Immunol*. 2004; 173:3916–3924. [PubMed: 15356140]
18. Chakravarty S, Herkenham M. Toll-like receptor 4 on nonhematopoietic cells sustains CNS inflammation during endotoxemia, independent of systemic cytokines. *J Neurosci*. 2005; 25:1788–1796. [PubMed: 15716415]
19. Teng W, Wang L, Xue W, Guan C. Activation of TLR4-Mediated NF $\kappa$ B Signaling in Hemorrhagic Brain in Rats. *Mediators of Inflammation*. 2009; 2009
20. Caso JR, Pradillo JM, Hurtado O, et al. Toll-like receptor 4 is involved in brain damage and inflammation after experimental stroke. *Circulation*. 2007; 115:1599–1608. [PubMed: 17372179]
21. Nakamura T, Xi G, Hua Y, Schallert T, Hoff JT, Keep RF. Intracerebral hemorrhage in mice: model characterization and application for genetically modified mice. *Journal of Cerebral Blood Flow and Metabolism*. 2004; 24:487–494. [PubMed: 15129180]

22. Poltorak A, He X, Smirnova I, et al. Defective LPS signaling in C3H/HeJ and C57BL/10ScCr mice: mutations in Tlr4 gene. *Science*. 1998; 282:2085–2088. [PubMed: 9851930]
23. Li X, Blizzard KK, Zeng Z, et al. Chronic behavioral testing after focal ischemia in the mouse: functional recovery and the effects of gender. *Experimental Neurology*. 2004; 187:94–104. [PubMed: 15081592]
24. Wahl F, Allix M, Plotkine M, Boulu RG. Neurological and behavioral outcomes of focal cerebral ischemia in rats. *Stroke*. 1992; 23:267–272. [PubMed: 1561657]
25. Wilson EH, Wille-Reece U, Dzierszynski F, Hunter CA. A critical role for IL-10 in limiting inflammation during toxoplasmic encephalitis. *J Neuroimmunology*. 2005; 165:63–74. [PubMed: 16005735]
26. Wagner KR. Modeling intracerebral hemorrhage: glutamate, nuclear factor-kappa B signaling and cytokines. *Stroke*. 2007; 38:753–758. [PubMed: 17261732]
27. Loftspring MC, McDole J, Lu A, et al. Intracerebral hemorrhage leads to infiltration of several leukocyte populations with concomitant pathophysiological changes. *J Cereb Blood Flow Metab*. 2009; 29:137–143. [PubMed: 18827833]
28. Vogl T, Tenbrock K, Ludwig S, et al. Mrp8 and Mrp14 are endogenous activators of Toll-like receptor 4, promoting lethal, endotoxin-induced shock. *Nat Med*. 2007; 13:1042–1049. [PubMed: 17767165]
29. Adair-Kirk TL, Senior RM. Fragments of extracellular matrix as mediators of inflammation. *Int J Biochem Cell Biol*. 2008; 40:1101–1110. [PubMed: 18243041]
30. Fong AM, Robinson LA, Steeber DA, et al. Fractalkine and CX3CR1 mediate a novel mechanism of leukocyte capture, firm adhesion, and activation under physiologic flow. *J Exp Med*. 1998; 188:1413–1419. [PubMed: 9782118]
31. Kanazawa N, Nakamura T, Tashiro K, et al. Fractalkine and macrophage-derived chemokine: T cell-attracting chemokines expressed in T cell area dendritic cells. *Eur J Immunol*. 1999; 29:1925–1932. [PubMed: 10382755]
32. Huang D, Shi FD, Jung S, et al. The neuronal chemokine CX3CL1/fractalkine selectively recruits NK cells that modify experimental autoimmune encephalomyelitis within the central nervous system. *FASEB J*. 2006; 20:896–905. [PubMed: 16675847]
33. Hughes PM, Botham MS, Frentzel S, et al. Expression of fractalkine (CX3CL1) and its receptor, CX3CR1, during acute and chronic inflammation in the rodent CNS. *Glia*. 2002; 37:314–327. [PubMed: 11870871]
34. Lyons A, Lynch AM, Downer EJ, et al. Fractalkine-induced activation of the phosphatidylinositol-3 kinase pathway attenuates microglial activation in vivo and in vitro. *J Neurochem*. 2009; 110:1547–1556. [PubMed: 19627440]
35. Zujovic V, Benavides J, Vige X, et al. Fractalkine modulates TNF-alpha secretion and neurotoxicity induced by microglial activation. *Glia*. 2000; 29:305–315. [PubMed: 10652441]
36. Zujovic V, Schussler N, Jourdain D, et al. In vivo neutralization of endogenous brain fractalkine increases hippocampal TNF-alpha and 8-isoprostane production induced by intracerebroventricular injection of LPS. *J Neuroimmunol*. 2001; 115:135–143. [PubMed: 11282163]
37. Mizuno T, Kawanokuchi J, Numata K, Suzumura A. Production and neuroprotective functions of fractalkine in the central nervous system. *Brain Res*. 2003; 979:65–70. [PubMed: 12850572]
38. Cardona AE, Pioro EP, Sasse ME, et al. Control of microglial neurotoxicity by the fractalkine receptor. *Nat Neurosci*. 2006; 9:917–924. [PubMed: 16732273]
39. Kong T, Choi JK, Park H, et al. Reduction in programmed cell death and improvement in functional outcome of transient focal cerebral ischemia after administration of granulocyte-macrophage colony-stimulating factor in rats. *Laboratory investigation*. *J Neurosurg*. 2009; 111:155–163. [PubMed: 19361262]
40. Nakagawa T, Suga S, Kawase T, Toda M. Intracarotid injection of granulocyte-macrophage colony-stimulating factor induces neuroprotection in a rat transient middle cerebral artery occlusion model. *Brain Res*. 2006; 1089:179–185. [PubMed: 16678804]

41. Schabitz WR, Kruger C, Pitzer C, et al. A neuroprotective function for the hematopoietic protein granulocyte-macrophage colony stimulating factor (GM-CSF). *J Cereb Blood Flow Metab.* 2008; 28:29–43. [PubMed: 17457367]
42. Kim NK, Choi BH, Huang X, et al. Granulocyte-macrophage colony-stimulating factor promotes survival of dopaminergic neurons in the 1-methyl-4-phenyl-1,2,3,6-tetrahydropyridine-induced murine Parkinson's disease model. *Eur J Neurosci.* 2009; 29:891–900. [PubMed: 19245369]
43. Zhao X, Sun G, Zhang J, et al. Hematoma resolution as a target for intracerebral hemorrhage treatment: role for Peroxisome Proliferator-Activated Receptor  $\gamma$  in microglia/macrophages. *Ann Neurol.* 2007; 61:352–362. [PubMed: 17457822]
44. Kunz A, Abe T, Hochrainer K, et al. Nuclear factor-kappaB activation and postischemic inflammation are suppressed in CD36-null mice after middle cerebral artery occlusion. *J Neurosci.* 2008; 28:1649–1658. [PubMed: 18272685]
45. Abe T, Shimamura M, Jackman K, et al. Key role of CD36 in Toll-like receptor 2 signaling in cerebral ischemia. *Stroke.* 2010; 41:898–904. [PubMed: 20360550]
46. Erdman LK, Cosio G, Helmers AJ, et al. CD36 and TLR interactions in inflammation and phagocytosis: implications for malaria. *J Immunol.* 2009; 183:6452–6459. [PubMed: 19864601]
47. Mikolajczyk TP, Skrzeczynska-Moncznik JE, Zarebski MA, et al. Interaction of human peripheral blood monocytes with apoptotic polymorphonuclear cells. *Immunology.* 2009; 128:103–113. [PubMed: 19689740]

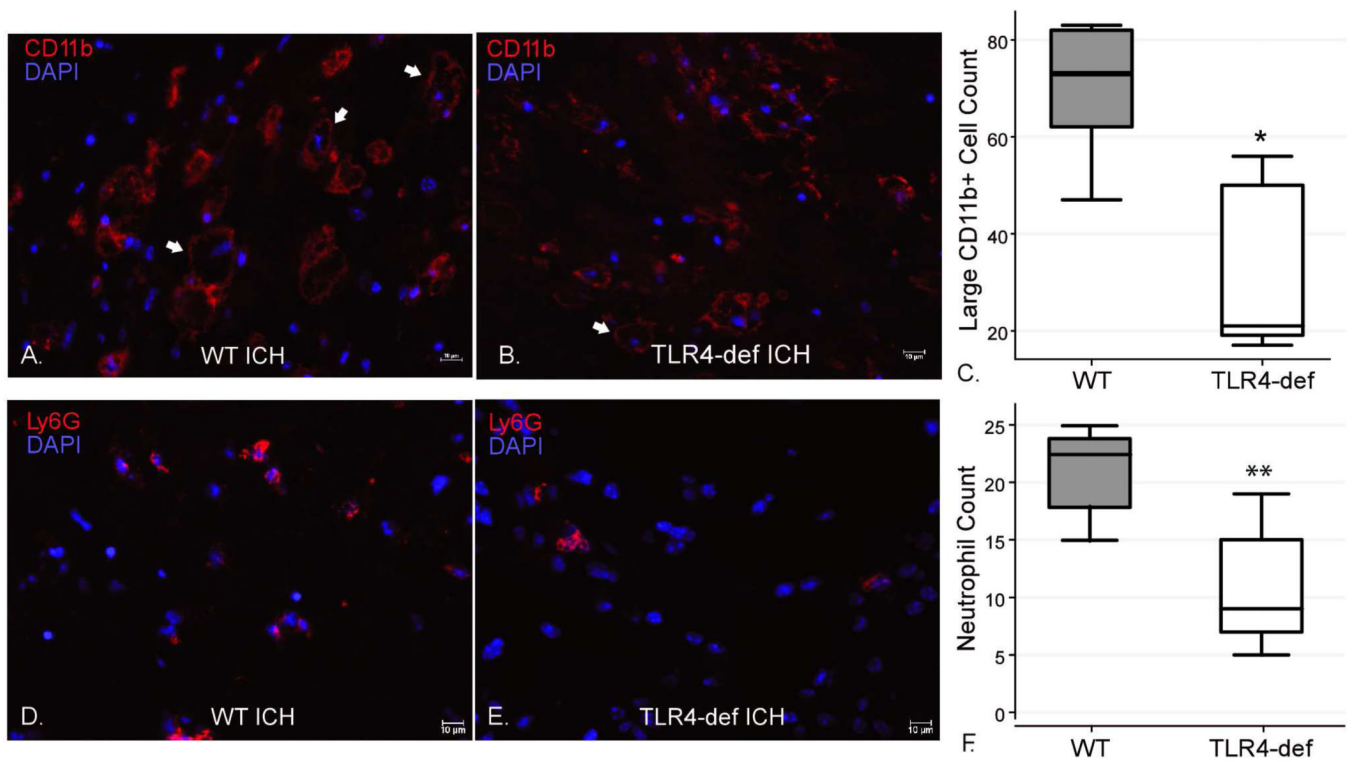


**Figure 1. Immunohistochemical staining for neutrophils and myeloid-derived cells 3 days after ICH surgeries in WT and TLR4-deficient mice**

(A–B) There was no significant difference between the genotypes in total numbers of CD11b<sup>+</sup> cells in five 20x fields (WT  $255.6 \pm 77.3$  cells vs. TLR4-deficient  $218.4 \pm 70.1$  cells,  $p=0.45$ ). However, there were more large, vacuolated CD11b<sup>+</sup> cells in the WT mice (representative cells indicated by arrows). (C) Boxplot of the number of large (>10  $\mu\text{m}$ ), vacuolated CD11b<sup>+</sup> cells in five 20x fields per mouse by genotype. \*  $p<0.05$ ,  $n=5/\text{genotype}$ . (D–E) Ly6G staining for neutrophils demonstrated more perihematomal neutrophils in the WT mice compared to TLR4-deficient mice. (F) Boxplot of numbers of perihematomal neutrophils in five 40x fields per mouse by genotype. \*\*  $p<0.01$ ,  $n=5/\text{genotype}$ . scale bar indicates 10  $\mu\text{m}$ .

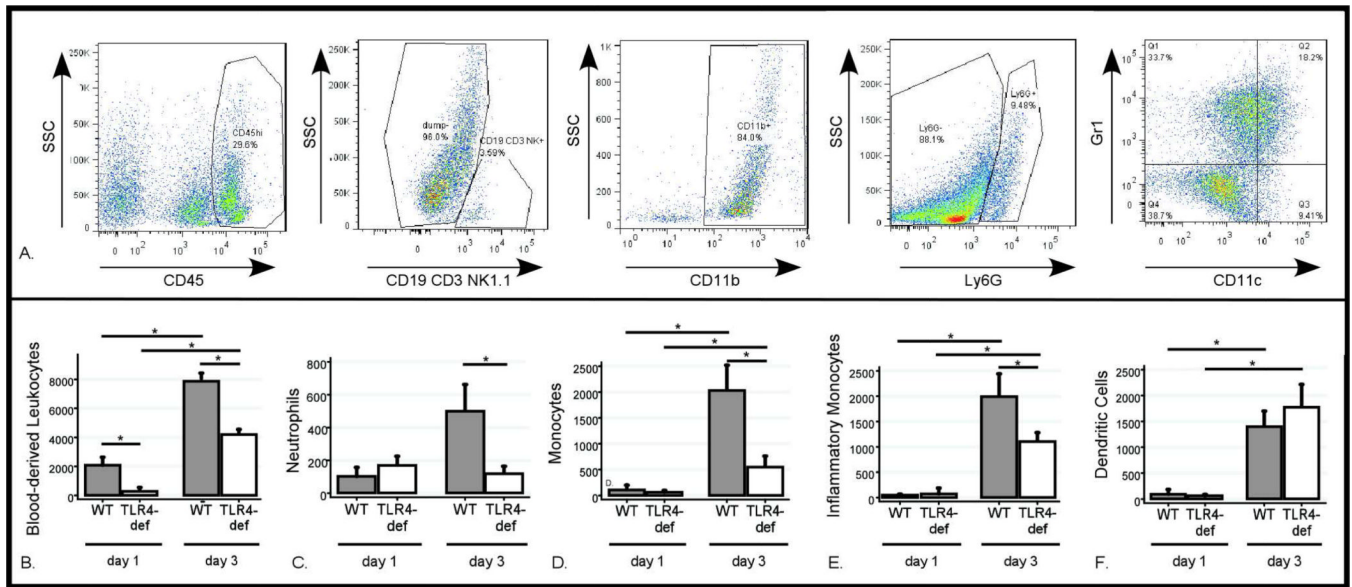


**Figure 2. Flow cytometric analysis of inflammatory infiltrate following ICH**

Brain flow cytometry results after ICH surgery. (A) Gating strategy of live cells to identify all blood-derived leukocytes (CD45<sup>hi</sup>), neutrophils (CD45<sup>hi</sup>CD3<sup>-</sup>CD19<sup>-</sup>NK1.1<sup>-</sup>CD11b<sup>+</sup>Ly6G<sup>+</sup>), monocytes (CD45<sup>hi</sup>CD3<sup>-</sup>CD19<sup>-</sup>NK1.1<sup>-</sup>CD11b<sup>+</sup>Ly6G<sup>-</sup>CD11c<sup>-</sup>GR1<sup>-</sup>), inflammatory monocytes (CD45<sup>hi</sup>CD3<sup>-</sup>CD19<sup>-</sup>NK1.1<sup>-</sup>CD11b<sup>+</sup>Ly6G<sup>-</sup>CD11c<sup>+</sup>GR1<sup>+</sup>) and dendritic cells (CD45<sup>hi</sup>CD3<sup>-</sup>CD19<sup>-</sup>NK1.1<sup>-</sup>CD11b<sup>+</sup>Ly6G<sup>-</sup>CD11c<sup>+</sup>). (B–F) Differences in each cell population between days 1 and 3 post-ICH in WT and TLR4-deficient mice. Data expressed as mean ± SEM excess ipsilateral cells, \* = p < 0.05 with correction for multiple comparisons, n = 4 / genotype on day 1 post-ICH and n = 6 / genotype on day 3 post-ICH.



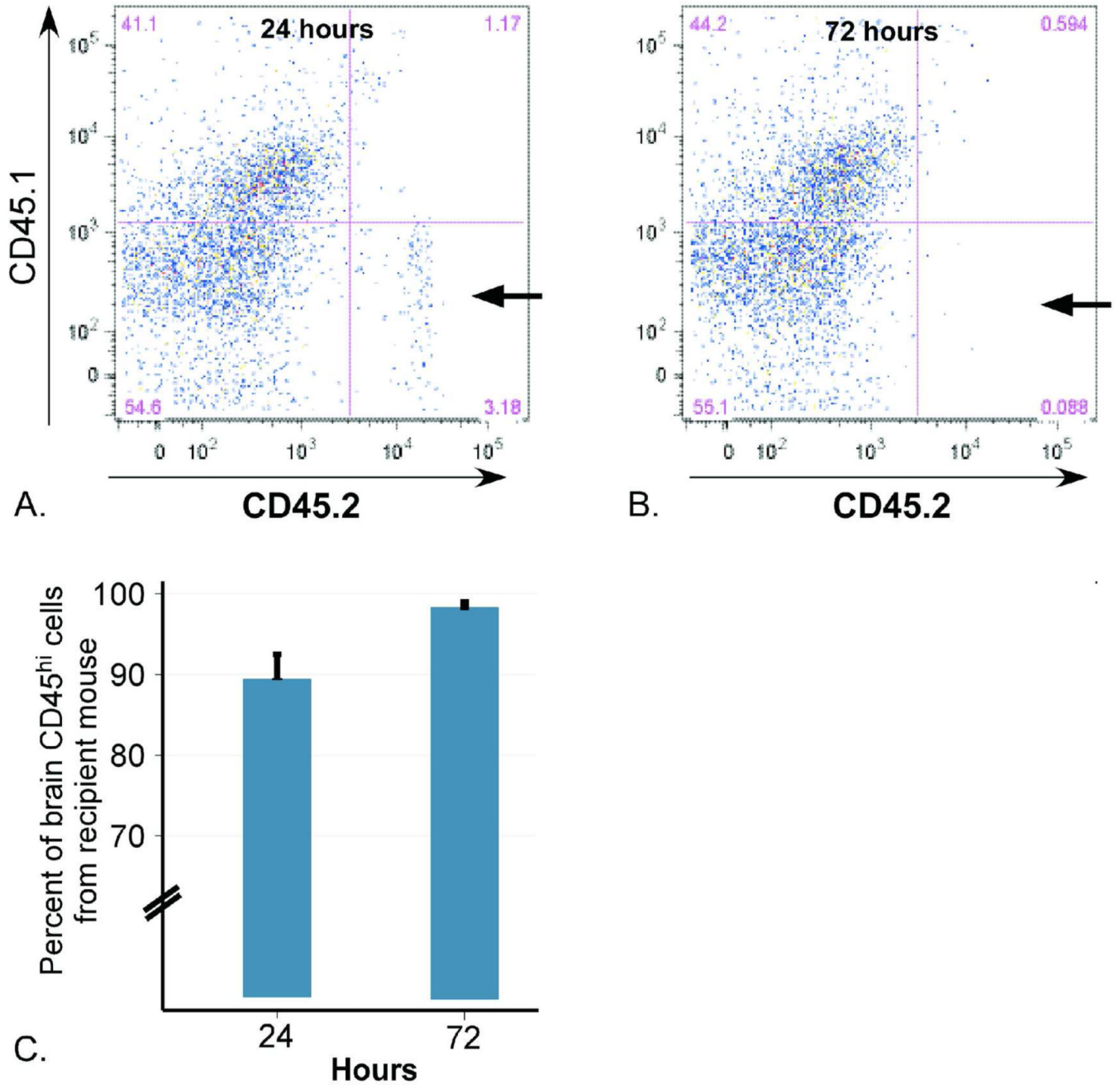


**Figure 3. Source of perihematomal leukocytes on post-ICH days 1 and 3**

Injection of blood from C57BL/6 mice (homozygous for the pan-leukocyte marker CD45.2) into B6LY5.2/Cr mice (homozygous for CD45.1) revealed that the majority of leukocytes quantified by flow cytometry originate from the recipient mouse. (A) Representative plot demonstrating only 3.2% of live cells staining positive for CD45.2 (arrow) at day 1 post-ICH, indicating their origin from the injected ICH. (B) At day 3 post-ICH, less than 0.1% of live cells are CD45.2<sup>+</sup> (arrow). (C) Quantification of percent of ipsilateral CD45<sup>+</sup> cells deriving from the recipient mouse (CD45.1<sup>+</sup>) at each time point.

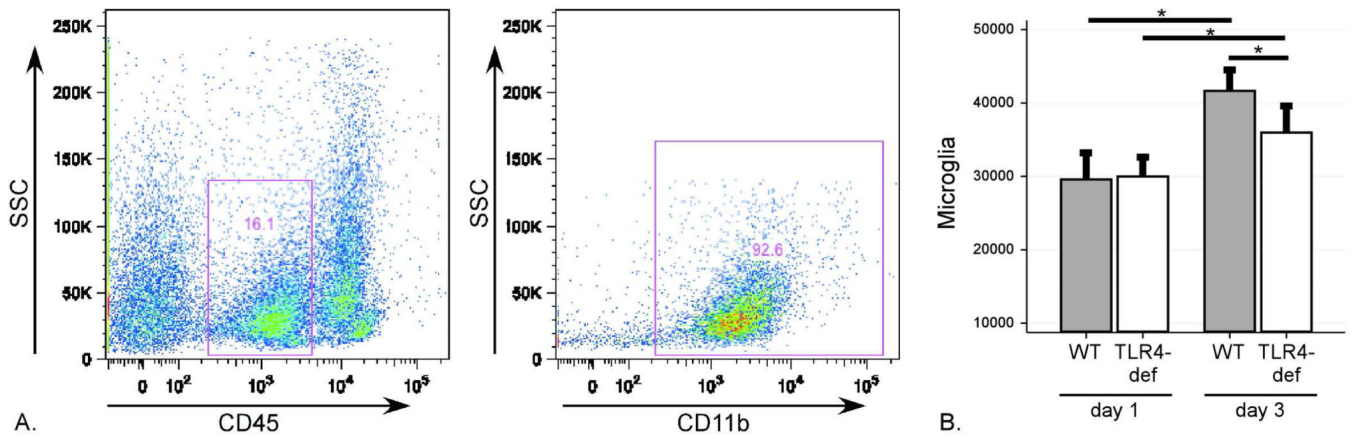


#### Figure 4. Flow cytometric analysis of microglia after ICH

Brain flow cytometry results after ICH surgery revealed a distinct microglial population. (A) Gating strategy to identify CD45<sup>int</sup>CD11b<sup>+</sup> cells identified as microglia. (B) Quantification of microglia counts on post-ICH days 1 and 3 in WT and TLR4-deficient mice. Data expressed as mean  $\pm$  SEM excess ipsilateral cells, \* =  $p < 0.05$  with correction for multiple comparisons,  $n = 4$  / genotype on day 1 post-ICH and  $n = 6$  / genotype on day 3 post-ICH.

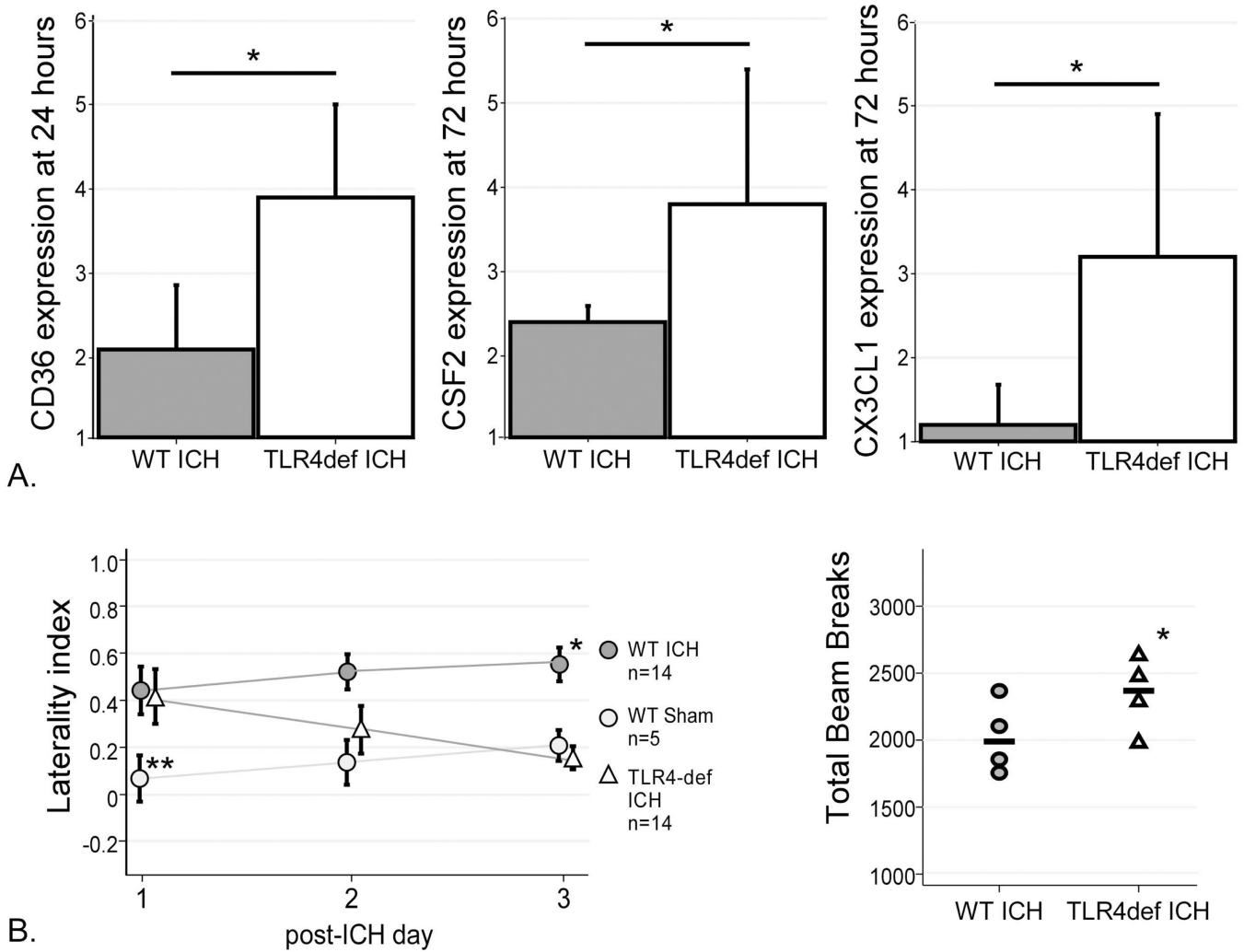


**Figure 5. Gene expression and Functional outcomes in WT and TLR4-deficient mice**  
 (A) TLR4-deficient mice had higher expression of CD36 at 24 hours, higher CSF2 expression at 72 hours, and higher CX3CL1 expression at 72 hours. n= 3 in each group, \* = p<0.05. (B) Cylinder test results for mice after sham (WT) and ICH surgeries (WT and TLR4-deficient). WT mice developed progressive left hemiparesis over 3 days after ICH surgery, while the TLR4-deficient mice improved. By day 3 post-ICH, the TLR4-deficient mice had significantly better left forelimb use than WT mice (p=0.01) and were not statistically different from sham (p=0.83). Open field testing revealed greater motility in the TLR4-deficient mice as indicated by higher numbers of total beam breaks in the 20 minute testing period. \* = p<0.05, \*\*=p<0.005.

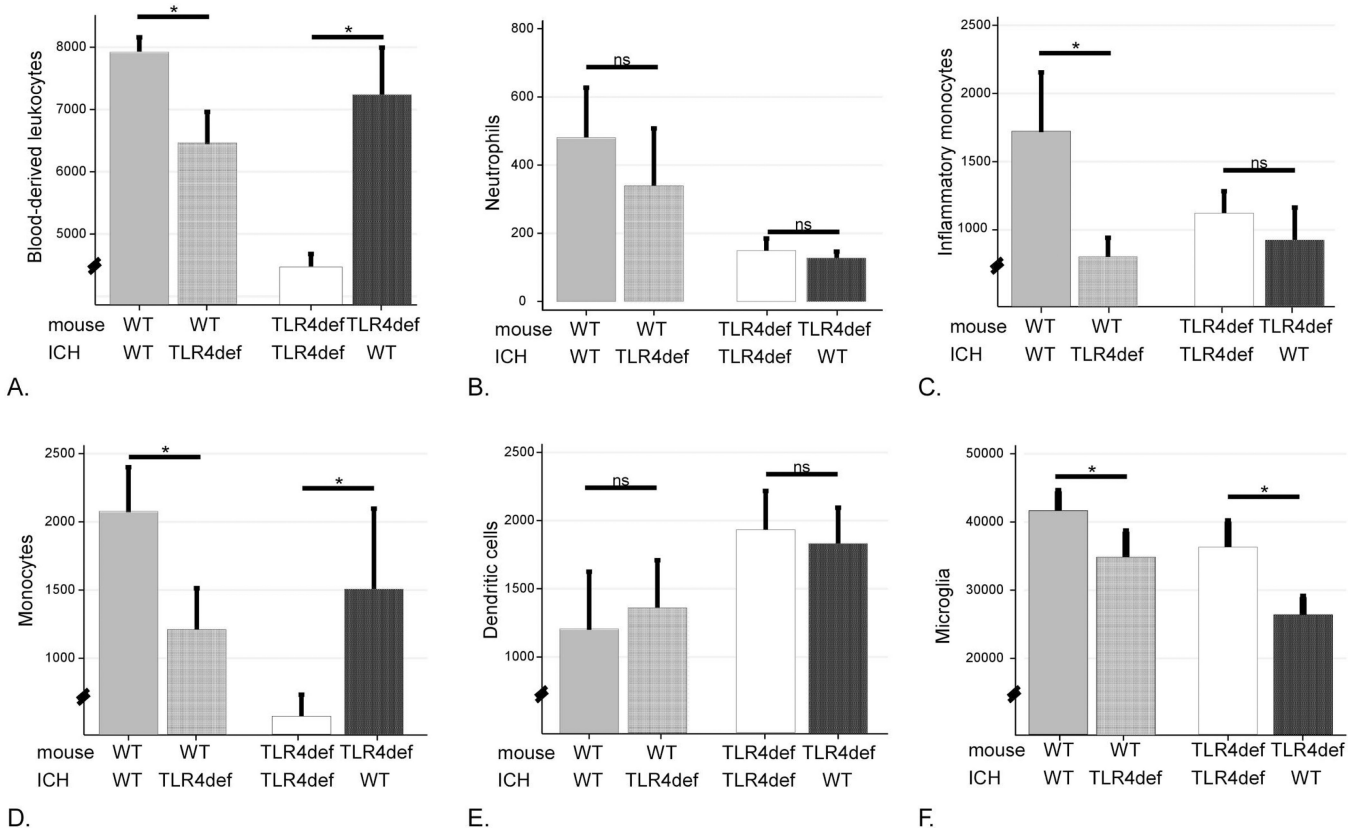


**Figure 6. Quantification of brain leukocyte populations after blood transfer experiments**  
 Creating ICH with blood from a donor mouse of the opposite genotype altered the composition of the inflammatory cells in the ipsilateral hemisphere. (A) Total blood-derived leukocytes were reduced in the WT mice with a TLR4-deficient ICH and increased in the TLR4-deficient mice given a WT ICH. (B) Neutrophil counts were not altered by the blood transfer. (C) Inflammatory monocytes were reduced in the WT mice with TLR4-deficient ICH. (D) Similar to total leukocytes, monocytes were reduced in the WT mice with a TLR4-deficient ICH and increased in the TLR4-deficient mice given a WT ICH. (E) Dendritic cell counts were not affected by the blood transfer. (F) Microglia counts were reduced in both the WT mice given a TLR4-deficient ICH and the TLR4-deficient mice given a WT ICH. n=6-7/group, \* p<0.05.

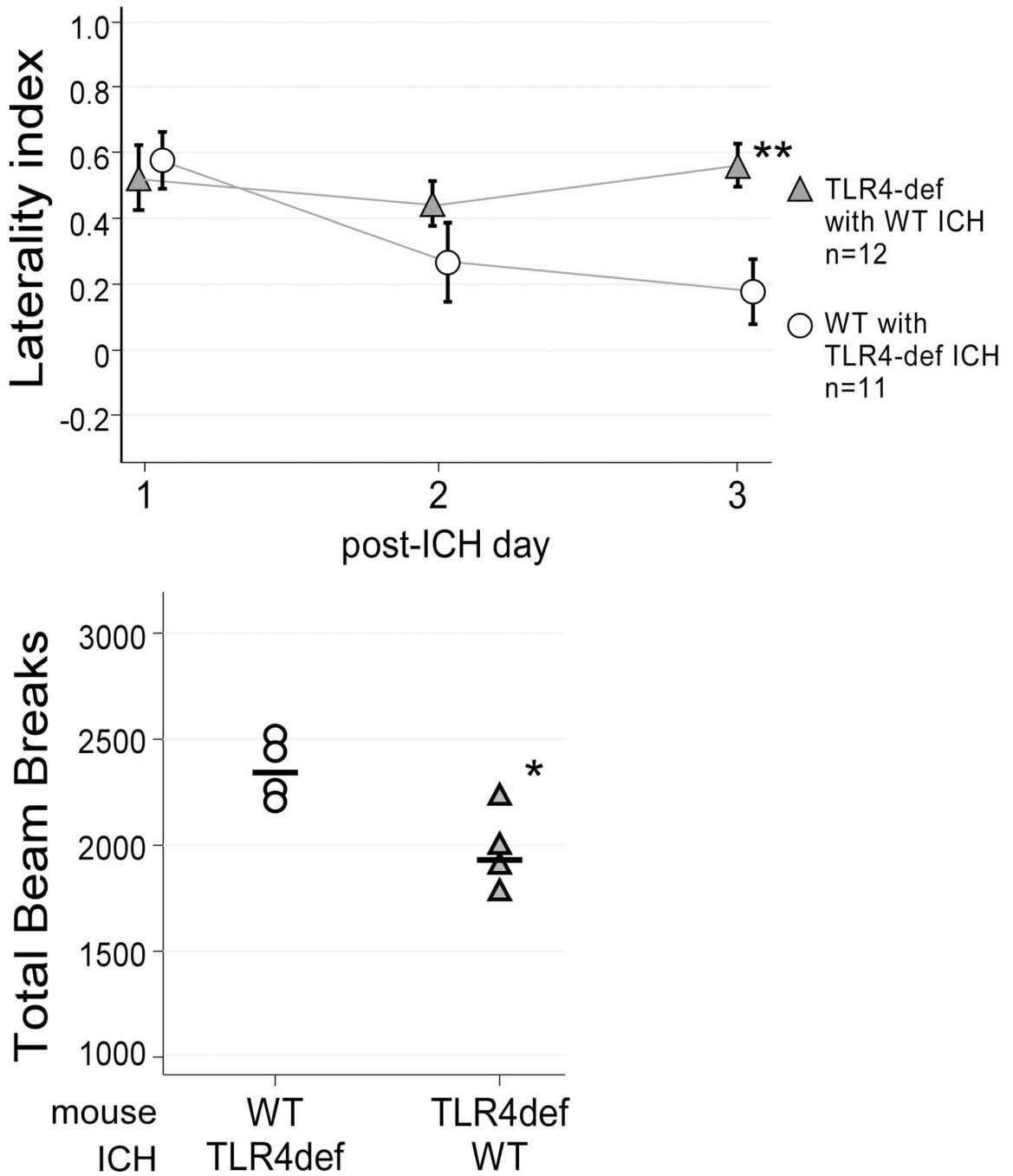


**Figure 7. Functional outcome after ICH blood transfer experiments**

Cylinder testing revealed WT mice with an ICH comprised of TLR4-deficient blood and TLR4-deficient mice with a WT ICH had the same functional impairment on day 1 post-ICH. WT mice with TLR4-deficient ICH improved over the 3 days post-ICH, similar to the TLR4-deficient mice with autologous ICH, while the TLR4-deficient mice with WT ICH worsened. \*\* $p < 0.005$ . Consistent with the cylinder testing results, open field testing on day 3 post-ICH revealed greater locomotor activity in the WT mice with a TLR4-deficient ICH,  $n = 4/\text{group}$ , \*  $p < 0.05$ .



**Table 1**

Systemic leukocyte differentials in peripheral blood and spleen in the TLR4-deficient and WT mice three days after ICH. Leukocytes expressed as percentage of total CD45<sup>hi</sup> cells, n=5 per group, n.s. = not significant.

|                         | Neutrophils (%) | Dendritic Cells (%) | Inflammatory Monocytes (%) | Monocytes (%)    |
|-------------------------|-----------------|---------------------|----------------------------|------------------|
| <b>Peripheral Blood</b> |                 |                     |                            |                  |
| WT ICH                  | 7.6 ± 0.7       | 1.7 ± 0.9           | 2.8 ± 1.8                  | 2.1 ± 0.8        |
| TLR4-deficient ICH      | 8.9 ± 2.7       | 0.7 ± 0.2           | 4.8 ± 4.0                  | 1.9 ± 0.8        |
| p                       | n.s.            | n.s.                | n.s.                       | n.s.             |
| <b>Spleen</b>           |                 |                     |                            |                  |
| WT ICH                  | 1.7 ± 0.5       | 1.6 ± 0.8           | 0.5 ± 0.3                  | <b>0.9 ± 0.5</b> |
| TLR4-deficient ICH      | 2.2 ± 0.8       | 2.6 ± 1.3           | 1.0 ± 0.4                  | <b>2.9 ± 0.5</b> |
| p                       | n.s.            | n.s.                | n.s.                       | <b>&lt; 0.05</b> |